JOURNAL OF Materials CHEMISTRY

Construction of organic–inorganic hybrid ultrathin films self-assembled from poly(thiophene-3-acetic acid) and TiO_2

Hanming Ding,*† Manoj Kumar Ram† and Claudio Nicolini

Department of Biophysical M&O Sciences and Technologies, Genoa University, Corso Europa 30, 16132 Genoa, Italy. E-mail: ding@yifan.net

Received 12th April 2002, Accepted 10th June 2002
First published as an Advance Article on the web 15th October 2002

Ultrathin films of poly(thiophene-3-acetic acid) (PTAA)/TiO_2 nanocomposite were fabricated layer by layer at various solid surfaces by consecutively adsorbing PTAA and $TiCl_4$ (in toluene–ethanol). The fabrication process was carried out by performing the controlled hydrolysis and condensation processes in separate steps. The build-up of such multilayer films was monitored by UV–VIS spectroscopy and quartz crystal microbalance measurements. The ordered multilayers were subsequently characterized by IR spectroscopy, atomic force microscopy, electrochemical, photo-electrochemical and electrical conductivity measurements. The potential application of such nanocomposite films in photovoltaic applications is discussed.

Introduction

There is increased interest in solar energy conversion by employing all or partly organic materials owing to their reduced size, light weight, low-temperature processing and low-cost large-area manufacture. For photovoltaic cells made with pure conducting polymers, energy conversion efficiencies were too low (typically 10^{-3}–10^{-2} %) to be used in practical applications.[1,2] An encouraging breakthrough for higher efficiencies is achieved by mixing electron-donor conducting polymers with suitable electron-acceptors.[3,4] By forming a single-layer blend, a phase-separated donor–acceptor (D–A) 'bulk heterojunction' is achieved between the donors and acceptors.[3] The interpenetrating D–A composites would appear to be ideal photovoltaic materials, since any point in the composite is within a few nanometers of a D–A interface.

Titanium dioxide (TiO_2) is an n-type inorganic semiconductor and a very promising material for photovoltaic applications. For example, dye-sensitized TiO_2 semiconductorsor Grätzel-type solar cells have an efficiency conversion of about 10%.[5] By incorporating TiO_2 with p-type conducting polymers, organic–inorganic (O–I) composite materials can be formed to improve their mechanical, electrical and optical properties.[6] These composite materials have attracted interest in both fundamental studies and applications: inorganic semiconducting nanoparticles for their small size and novel properties, and conjugated polymers for their attributes as easily processed semiconductor materials with potential in optoelectronic applications.[7,8] In such O–I composite materials, a p–n interface can be formed at the nanometer scale. For optoelectronic applications, the conjugated polymers in most cases are polythiophene, poly(*p*-phenylene vinylene), polypyrrole, polyaniline and their derivatives. Nanoparticles include CdSe or CdS, TiO_2, $BaTiO_3$, SiO_2, Fe_2O_3, *etc.*[9–19] The mostly used methods for the formation of composites are mechanical blending to form single-layer blends and spin-coating to form double-layer structures, *i.e.*, one-layer nanoparticles and one-layer conducting polymers.

However, in photovoltaic applications, single-layer structures blended from conducting polymers and inorganic nanoparticles limit the occurrence of charge transfer, and easily results in charge buildup on a single site. Due to the molecular nature of the charge separation process, efficient charge separation occurs only at the D–A (or p–n) interface in double-layer structures. Thus, double-layer structures will also limit the photovoltaic conversion efficiency.[20] To realize the full potential in the photovoltaic applications, it is highly desirable to endow careful design of the O–I nanocomposites. It is well known that an inorganic alkoxide can react directly with a polymer or an oligomer having appropriate functional groups, thus providing covalent linkages between the organic phase and the inorganic network.[21–25] Based on this idea, metal oxide films and molecules with hydroxy groups can be grown layer by layer, by performing controlled hydrolysis and condensation reactions in separate steps. Since the composition, thickness and orientation of each layer in layer-by-layer (LBL) films can be manipulated at the molecular level, this provides a new route for the formation of layered nanocomposite structures.[26–34]

In the present paper, by employing poly(thiophene-3-acetic acid) (PTAA) and $TiCl_4$ (in toluene–ethanol), we have fabricated multilayer p–n hetero-junctions in conducting PTAA/TiO_2 LBL ultrathin films, and measured their electrical, electrochemical and photo-electrochemical properties.

Experimental section

Poly(thiophene-3-acetic acid) (PTAA) was synthesized by ferric chloride polymerization of ethyl-3-thiopheneacetate followed by acid hydrolysis using the method similar to Royappa and Rubner's.[35] Titanium(IV) chloride (1.0 M solution in toluene) ($TiCl_4$), poly(diallyldimethylammonium chloride) (PDDA) (average molecular weight, 200,000–350,000, 20% wt. in water) and other chemicals used herein were purchased from Aldrich. Quartz plate, silicon wafer, mica, aluminium electrodes of the quartz crystal microbalance (QCM), indium–tin oxide (ITO)-coated glass plates and interdigitated electrodes were used as the substrates for the fabrication of LBL films. All the substrates were treated as hydrophilic according to the usual procedures and kept in deionized water prior to their use for LBL deposition.

PTAA was dissolved in 0.1 mol dm^{-3} NaOH at a concentration of 1 mg cm^{-3} and then sonicated for 12 h. The solution was then filtered with 7 μm filter paper to remove any trace of undissolved materials. Subsequently this solution was adjusted to acidic by slow addition of HCl. The pH effect was checked carefully for the pH dependence of the depositing

†Also affiliated with Polo Nazionale Bioelettronica-Genoa Section.

solution and the PTAA solution was carefully adjusted to pH 4.5. 50 mmol dm^{-3} $TiCl_4$ solution was prepared in 1 : 1 (v/v) toluene–ethanol. For these hydrophilic surfaces, the substrates were treated previously by being immersed in a 1.9 mmol dm^{-3} PDDA acidic solution (pH 1). The pre-treated substrates were immersed alternately in PTAA and $TiCl_4$ toluene–ethanol solutions and subsequently rinsed with acidic water and ethanol and then dried with nitrogen.

UV–VIS spectra were recorded using a V-570 UV–VIS–NIR spectrophotometer (Jasco, Japan). The LBL films were deposited on quartz slides and the spectra were collected in the wavelength range 200–800 nm. IR spectra were measured using a Bruker EQUINOX 55 IR spectrometer. The film sample was fabricated on a silicon wafer and the transmission method was employed. Atomic force microscope (AFM) imaging was performed in contact mode in ambient air with a homemade instrument. QCM samples were tested with a homemade nanogravimetric apparatus and a GFC-8010G frequency counter (Good Will Instrument Co., Taiwan). The electrical characterization was performed on interdigitated electrodes using a Keithley 6517 electrometer. The electrochemical measurements were carried out in a potentiostat/galvanostat (EG&G PARC, model 263A). A standard three-electrode configuration was used, where LBL films on an ITO glass plate acted as a working electrode, platinum as a counter, and Ag/Ag^+ as a reference electrode.

Results and discussion

The LBL films of PTAA and TiO_2 were prepared by sequential adsorption/hydrolysis/condensation, as outlined in Fig. 1. The driving force for fabrication of the LBL films is the interactions between carboxylic acid groups and titanium. When PTAA films were immersed into a $TiCl_4$ toluene–ethanol solution, since $TiCl_4$ reacts with ethanol, titanium chloro-ethoxides reacted with the carboxylic groups in PTAA and carboxylate groups were chelated to titanium. The activated TiO_2 surface was then attached to carboxylic groups when such a film was reimmersed in PTAA solution. The interfacial chelating bonds between carboxylate groups and titanium has been confirmed by IR and Raman spectroscopy.[36] Sulfonate groups show a similar interaction with titanium. For example, Shin *et al*. have successfully fabricated patterned TiO_2 films on hydrophilic sulfonate surfaces.[37] Thus, it is possible to fabricate LBL films using any molecules or polymers with substituted carboxylic, sulfonic or phosphate groups and some functional nanoparticles based on titanium, boron, zirconium, niobium or aluminium.[38–41]

UV–VIS spectroscopy and QCM were used to follow the growth of the LBL multilayers. UV–VIS absorption spectra following the growth of the PTAA/TiO_2 LBL films, up to 20 bilayers, are shown in Fig. 2, in which two absorption bands are observed at 240 and 400 nm. It can be easily deduced from the solid and dotted lines in Fig. 2, that the peak at 400 nm can be ascribed to the absorbance of polythiophene, while the band around 240 nm is attributable to TiO_2. The peak of PTAA has a small blue shift of about 10 nm relative to the absorption peak in PTAA/PDDA LBL films, and is similar to that of its

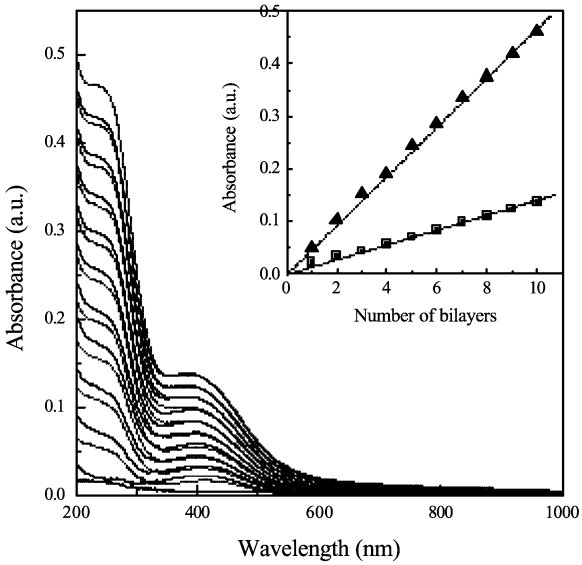

Fig. 2 UV–VIS absorption spectra of multilayers of PTAA/TiO_2 LBL films with different number of bilayers on a quartz plate. Inset: the absorbance magnitude at 250 and 400 nm as a function of the number of bilayers.

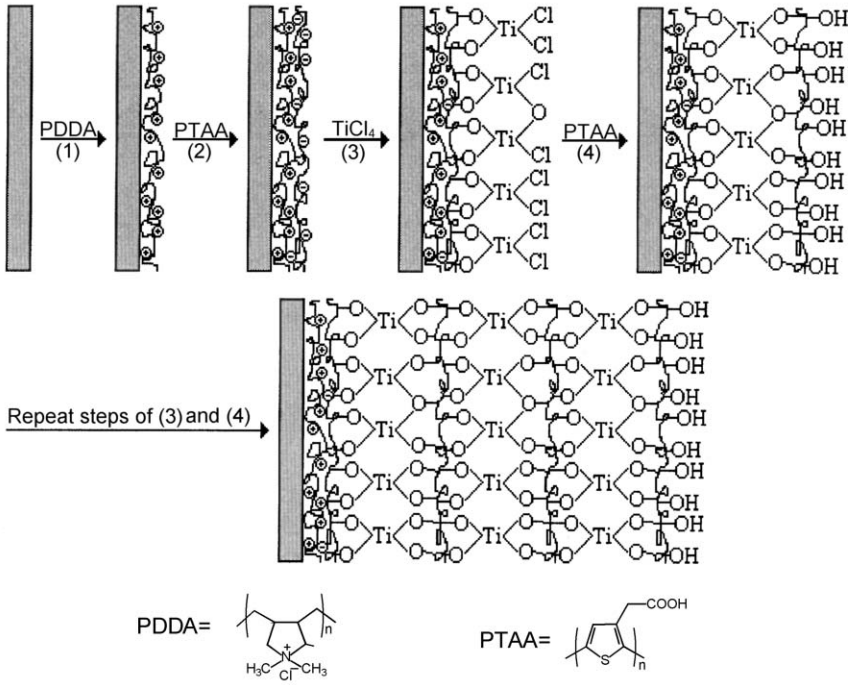

Fig. 1 Schematic of fabrication of multilayers of PTAA/TiO_2 nanocomposites.

aqueous solution. The position of this peak is associated with molecular structure and the stereoconformation of PTAA in films. The peak of TiO_2 shifts to lower wavelength and reaches a steady value at 240 nm with increase in the deposited layers. It is well known that the optical spectra of semiconductor particles show a blue shift as the size of particles decrease. In rutile or anatase TiO_2 particles, the onset of optical absorption of bulk TiO_2 is at $\lambda = 385$ nm for the anatase phase and $\lambda = 415$ nm for rutile phase. For $\lambda = 240$ nm, the calculated bandgap shift of the TiO_2 particles in the LBL films is then 1.95 or 2.18 eV, as compared to bulk anatase or rutile, respectively. A mathematical treatment using a quantum mechanical approach yields a relationship between bandgap shift (ΔE_g) and radius (R) of quantum-size particles, expressed as[42]

$$\Delta Eg = \frac{h^2}{8R^2}\left[\frac{1}{m_e^*} + \frac{1}{m_h^*}\right] - \frac{1.8e^2}{\varepsilon R}$$

Here h is Planck's constant, m_e* and m_h* are the electron and hole effective mass respectively, e is the electron charge, and ε is the dielectric constant of the semiconductor. Taking reported values of $\varepsilon = 184$ and $1/m_e^* + 1/m_h^* = 0.63\ m_e$ (m_e is the electron rest mass) for TiO_2 semiconductor,[43] the diameter of TiO_2 nanoparticle in LBL films is estimated as $2R = 1.0$ nm. It is clear that very small TiO_2 nanoparticles are incorporated into the PTAA polymer matrixes. The fabrication process results in increased surface area per unit volume of TiO_2 and molecular contact between PTAA and TiO_2 nanoparticles. Thus, based on this LBL method, multi-layered nanocomposite structures can be formed.

It can be seen in the inset of Fig. 2 that the absorption magnitude at 240 and 400 nm increases linearly with the number of bilayers of the LBL films, yielding an average optical density of 0.0138 $\pm$ 0.0002 (at 240 nm) or 0.0470 $\pm$ 0.0005 (at 400 nm) per bilayer. These linear features suggest that each layer contributes an equal amount of material to the thin films for TiO_2 or PTAA, respectively. As shown in Fig. 2, the consecutive adsorption of layers is stepwise, and the fabrication process is linear and consistent for both TiO_2 and PTAA.

The fabrication process was also monitored by a QCM with aluminium electrode, with a sensitivity is 0.018 ng Hz^{-1} mm^{-2}.[44] Based on the Sauerbrey equation,[45] the film thickness on a QCM electrode shows a relationship with the film density as follows:

$$2d\ (\text{nm}) = -0.018^*\Delta F\ (\text{Hz})/\rho\ (\text{g cm}^{-3})$$

Using the bulk density of a TiO_2-based gel (1.7 g cm^{-3}),[25] a ΔF value of 200 $\pm$ 38 Hz corresponds to a thickness of 1.1 $\pm$ 0.2 nm for the TiO_2 layer. The value is analogous to the thickness of the TiO_2 layer between poly(acrylic acid) layers (1.4 $\pm$ 0.4 nm).[40] This result indicates that the TiO_2 layers are essentially single layers of TiO_2 nanoparticles because the diameter of the nanoparticles is about 1.0 nm based on UV–VIS measurement. The frequency change of PTAA layer is also regular, 77 $\pm$ 20 Hz per bilayer. The linear frequency decrease in QCM measurements also reveals the regular growth of PTAA/TiO_2 multilayers on the aluminium electrode.

Fig. 3 shows the IR spectrum of a 40-bilayer PTAA/TiO_2 nanocomposite LBL film on a silicon wafer. The bands at 1556 and 1420 cm^{-1} correspond to the asymmetric and symmetric stretching vibrations of the carboxylate groups. This suggests that some carboxylic groups in PTAA exist as their carboxylate anions in the LBL films. The band at 1108 cm^{-1} may be ascribed to the vibration of the thiophene five-atom ring or Ti–O–Ti or Ti–O–C vibrations. Since, however, there is no strong band around 1200–1000 cm^{-1} for thiophene-3-acetic acid, the strong band at 1108 cm^{-1} is mostly attributable to Ti–O–Ti or Ti–O–C vibrations.[46] This evidence indicates that the carboxylic groups of PTAA are chelated to titanium. The existence

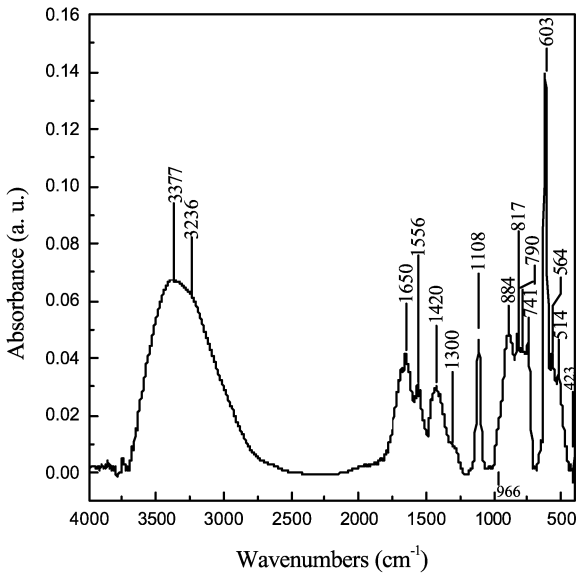

Fig. 3 FTIR spectrum of a 40-bilayer PTAA/TiO_2 LBL film on a silicon wafer.

of the Ti–O–Ti network is evidenced by the very strong band at 603 cm^{-1} and other bands ranging from 600 to 400 cm^{-1}. The bands around 1000–700 cm^{-1} mainly arise from C–C or C–S vibrations in the thiophene aromatic ring. The appearance of two bands at 3377 and 3236 cm^{-1} reveals the presence of –OH stretching vibrations in the LBL films. The band located at 1650 cm^{-1} arises from the vibration mode of free carboxylic acid groups. These three bands reveal that there are still some free carboxylic groups in the LBL films. Since the intensity of the peak at 1650 cm^{-1} is larger than the stretching modes of the bound carboxylate groups, most of carboxylic groups are expected to be free in the LBL films with the remainder covalently bound to titanium in the TiO_2 layer. In order to ascertain the stability of the chelating interaction between carboxylic groups in PTAA and TiO_2, the LBL films were illuminated under intense white light for 30 min. The IR spectrum of such illuminated films is similar to that without illumination suggesting that the chelating interaction is stable under light illumination.

Fig. 4 shows an AFM image of a one-bilayer nanocomposite LBL film deposited on mica (TiO_2 on the outermost layer). The TiO_2 layer exhibits a microscopic structure formed from small, nanometer-scale grains with uniformity in the film. The AFM image shows fine grains, with particle size varying from 3 to 15 nm in diameter. This size is a little larger than that estimated by the quantum mechanical method. This is due to the fact that the TiO_2 nanoparticles readily aggregate (UV–VIS spectra were

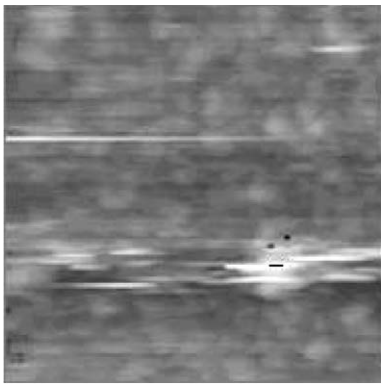

Fig. 4 AFM image of a one-bilayer PTAA/TiO_2 LBL film (TiO_2 on the outermost layer). The dimension of the image is 125 nm $\times$ 125 nm.

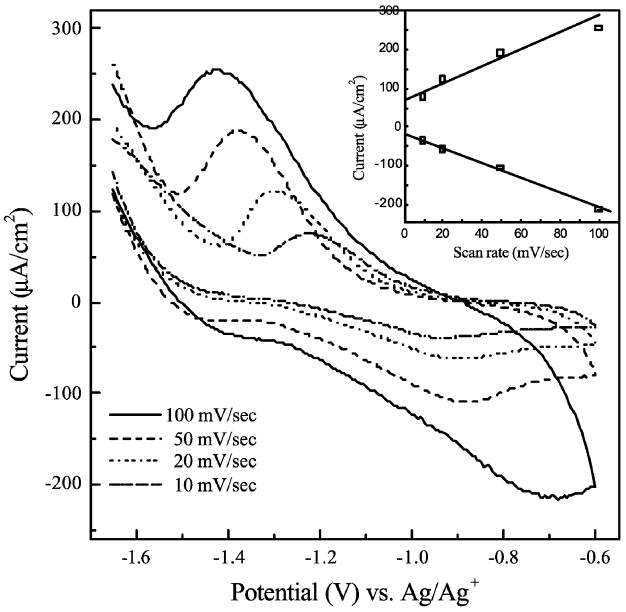

Fig. 5 Cyclic voltammograms of a 20-bilayer PTAA/TiO_2 LBL film on an ITO glass plate at different scan rates: (a) 100, (b) 50, (c) 20 and (d) 10 mV s^{-1}. The electrolyte is 0.1 mol dm^{-3} NBu_4BF_4 acetonitrile solution.

measured immediately after deposition, while the AFM image was recorded after one week). The morphological investigation of the PTAA layer shows a granular morphology similar to other classes of LBL films.[34]

Cyclic voltammetry was performed to characterize the LBL films. Fig. 5 shows cyclic voltammograms (CVs) of PTAA/TiO_2 nanocomposite LBL films in 0.1 mol dm^{-3} tetrabutylammonium tetrafluoroborate (NBu_4BF_4) acetonitrile solution at various scan rates. The CV shows two oxidation peaks at –1475 and –880 mV, and a reduction peak at –1376 mV *vs.* an Ag/Ag^+ reference electrode. For PTAA LBL films, the CV only shows an oxidation peak around 80 mV (at 50 mV s^{-1}), which originates from the thiophene ring. Owing to the interaction between carboxylate groups and TiO_2 nanoparticles, the electrons easily flow from PTAA to TiO_2. Accompanying the oxidation of the thiophene ring in PTAA, an electron moves from the thiophene ring to TiO_2 through the carboxylate group.[47] As redox processes occur between PTAA and TiO_2 nanoparticles, PTAA/TiO_2 LBL films show a distinct electrochemical behavior from PTAA LBL films. The currents of the oxidation peak at –880 mV and reduction peak at −1376 mV are directly proportional to the square root of scan rate over the range 10–100 mV s^{-1}, indicating that the LBL film is a surface-confined species and diffusion controlled system. The calculated diffusion coefficients are 8.24×10^{-10} cm^2 s^{-1} for both the oxidation and reduction processes, according to Randles–Sevcik equation, when one electron is expected to participate in the reaction mechanism of the composite system. Chronoamperometric measurement shows that the oxidation and reduction response time was <5 ms (as shown in Fig. 6). This fact suggests that the insertion of electrolyte ions into the nanocomposite LBL films is very fast and easy.

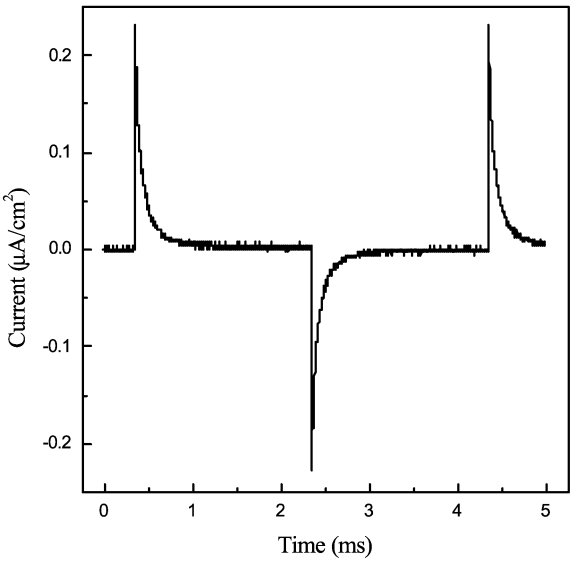

Fig. 6 Oxidation and reduction current responses of a 20-bilayer PTAA/TiO_2 LBL film.

Fig. 7(a) shows the current–voltage (*I–V*) response of a 20-bilayer PTAA/TiO_2 LBL film in an electrochemical cell in the dark and under light illumination. A distinct rectification behavior is found. According to the bandgap diagrams of polythiophene and TiO_2 (inset in Fig. 7(a)), the valence band of polythiophene is about 2.3 eV higher than the conduction band of TiO_2.[48] In reverse bias, electron-injection into PTAA and electron-removal from TiO_2 are energetically unfavorable. This

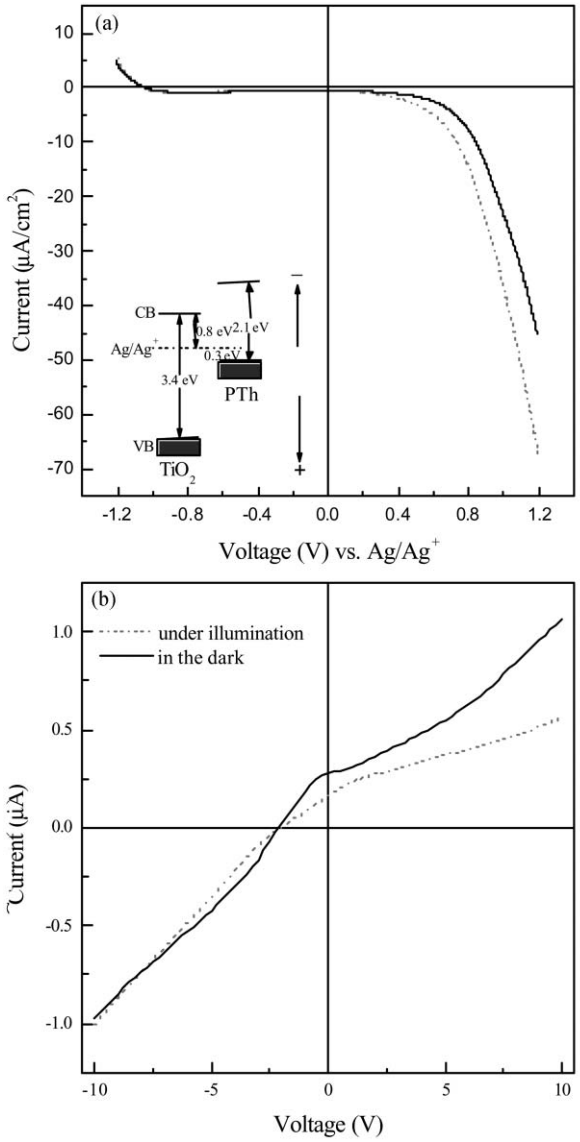

Fig. 7 (a) Current–voltage (*I–V*) characteristics of a 20-bilayer PTAA/TiO_2 LBL film on ITO glass in the dark (solid line) and under light illumination (dotted line). The electrolyte is 0.1 mol dm^{-3} NBu_4BF_4 acetonitrile solution. (b) Current–voltage (*I–V*) characteristics of a 20-bilayer PTAA/TiO_2 LBL film on an interdigitated electrode in the dark (solid line) and under light illumination (dotted line).

inherent polarity of the device results in very low current densities. On the other hand, electron-injection into TiO_2 and electron-removal from PTAA are energetically favorable, thus resulting in relatively high current densities under forward bias. Under light illumination, photoexcited electrons tend to flow from the PTAA layer to the conduction band of TiO_2. Here the p–n interface plays an important role in the enhancement of photocurrent.[3] In forward bias, the electron transfer process is energetically favorable and the current densities increase while in reverse bias, this process is suppressed by a reversed external electric field.

Fig. 7(b) shows the *I–V* characteristics of a 20-bilayer PTAA/TiO_2 LBL film deposited on an interdigitated electrode in the dark and under light illumination. In the dark, such films show a non-ohmic behavior, which is associated with the introduction of TiO_2 in the LBL films. By comparison, PTAA/PDDA LBL films on an interdigitated electrode show an ohmic behavior, with a conductivity is about 10^{-8} S cm^{-1}. Interestingly, under light illumination, the cathodic current remains unchanged, while the anodic current decreases. As the LBL films were deposited on the interdigitated electrode, the current flows inside the intra-layer (parallel direction) rather than the inter-layer (perpendicular direction). Under light illumination, in forward bias, the PTAA layer injects photoexcited electrons into the conduction band of the TiO_2, resulting in a decreased electron contribution to the parallel current in the PTAA layer. Therefore, the anodic current decreases, rather than increases. In reverse bias, the external electric field suppresses electron transfer from PTAA to TiO_2, so the cathodic current remains unchanged.

The photoelectrochemical response of the LBL films were evaluated using a three-electrode electrochemical cell in 0.1 mol dm^{-3} NBu_4BF_4 acetonitrile solution. A steady state electrochemical photocurrent was observed by applying potential from the potentiostat and the photocurrent was measured. Fig. 8 shows the photoelectrochemical response of a 20-bilayer PTAA/TiO_2 LBL film. The potential of the working electrode was set at 0.0 V *vs.* the Pt counter electrode. A fast and uniform photocurrent response was observed in each switch-on and switch-off condition, which is related to ion transport in the electrolyte, but is more dependent on the p–n interface in the nanocomposite films. The photocurrent is generated when photons are adsorbed by PTAA at the TiO_2/electrolyte interface, and subsequently electrons are injected into the conduction band of the TiO_2 nanoparticles.

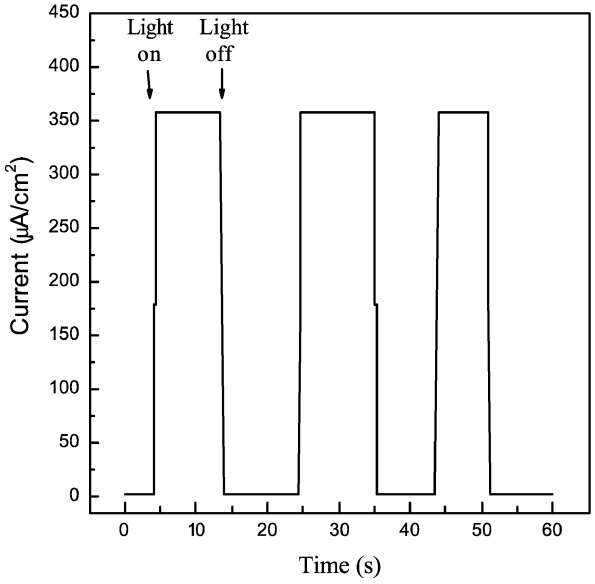

Fig. 8 Photoelectrochemical response of a 20-bilayer PTAA/TiO_2 LBL film in an electrolyte of 0.1 mol dm^{-3} NBu_4BF_4 acetonitrile solution. The potential of the working electrode was set at 0.0 V *vs.* the Pt counter electrode.

The sol–gel method described here offers a potentially powerful strategy for fabricating ordered conducting polymer/TiO_2 (or other semiconductor nanoparticles) multilayer ultrathin films on various substrates at ambient conditions. Manipulation at the molecular level results in truly molecular contact between conducting polymer and semiconductor nanoparticles. Such a nanocomposite forms interpenetrating phase-separated p–n hereto-junctions in the films, which would enhance the performances of some electronic or optoelectronic devices based on such nanocomposite thin films, for example, photovoltaic and electroluminescent devices.

Conclusions

In conclusion, we have fabricated LBL ultrathin films of PTAA/TiO_2 nanocomposites. PTAA acidic species and TiO_2 were fabricated onto various substrates by the layer-by-layer self-assembly technique. Both UV–VIS spectroscopy and QCM measurement show a uniform deposition process. UV–VIS spectroscopy as well as AFM images reveal that TiO_2 is dispersed in the polymeric films as very fine nanoparticles. IR spectroscopy indicates that some carboxylic groups of PTAA are bound to TiO_2 while the remainder are free in the LBL films. Electrochemical investigation shows that electrons can transfer from the thiophene ring to TiO_2 nanoparticles. Chronoamperometric measurement shows the redox processes are very fast. Current–voltage measurements demonstrate a rectification behavior both in the dark and under illumination in an electrochemical cell; but show an abnormal electrical behavior on an interdigitated electrode. Under light illumination such films displayed an increased photocurrent. By optimizing the preparation conditions and film parameters, such nanocomposite could be used in photovoltaic generation.

Acknowledgements

We thank Drs Marco Sartore, Marco Spinetti and Mario Panza for AFM measurements. Financial support from Edison Thermophotovoltaic S.p.a. and a MURST-PST contract to Polo Nazionale Bioelettronica are gratefully acknowledged.

References

1 G. Yu, C. Zhang and A. J. Heeger, *Appl. Phys. Lett.*, 1994, **64**(12), 1540.
2 H. Antoniadis, *Polym. Prepr.*, 1993, **34**(2), 490.
3 G. Yu, J. Gao, J. Hummelen, C. Wudl and A. J. Heeger, *Science*, 1995, **270**, 1789.
4 M. Granström, K. Petritsch, A. C. Arias, A. Lux, M. R. Andersson and R. H. Friend, *Nature*, 1998, **395**, 257.
5 M. Grätzel, K. Brooks and A. J. McEvoy, *Innovative Materials in Advanced Energy Technologies*, Farenza, Italy, 1999, p. 577.
6 A. P. Alivisatos, *Science*, 1996, **271**, 933.
7 G. Horowitz and F. Garnier, *Sol. Energy Mater.*, 1986, **13**, 47.
8 A. J. Frank, S. Glenis and A. J. Nelson, *J. Phys. Chem.*, 1989, **93**, 3818.
9 K. S. Narayan, A. G. Manoj, J. Nanda and D. D. Sarma, *Appl. Phys. Lett.*, 1999, **74**(68), 871.
10 A. C. Arango, S. A. Carter and P. J. Brock, *Appl. Phys. Lett.*, 1999, **74**(12), 1698.
11 S. A. Carter, J. C. Scott and P. J. Brock, *Appl. Phys. Lett.*, 1997, **71**(9), 1145.
12 Y. Hao, M. Yang, C. Yu, S. Cai, M. Liu, L. Fan and Y. Li, *Sol. Energy Mater. Sol. Cells*, 1998, **56**, 75.
13 P. R. Somani, R. Marimuthu, U. P. Mulik, S. R. Sainkar and D. P. Amalnerkar, *Synth. Met.*, 1999, **106**, 45.
14 D. S. Ginger and N. C. Greenham, *Synth. Met.*, 1999, **101**, 425.
15 G. Wang, H. Che, H. Zhang, C. Yuan, Z. Lu, G. Wang and W. Yang, *Appl. Surf. Sci.*, 1998, **135**, 97.
16 T. Cassagneau, T. E. Mallouk and J. H. Fendler, *J. Am. Chem. Soc.*, 1998, **120**, 7848.

17 P. Somani, B. B. Kale and D. P. Amalnerkar, *Synth. Met.*, 1999, **106**, 53.
18 M. Lira-Gautu and P. J. Gomez-Romero, *Solid State Chem.*, 1999, **147**, 601.
19 S. Patil, M. A. More, R. B. Gore, S. V. Rao and P. P. Patil, *Mater. Sci. Eng. B*, 1999, **65**, 145.
20 L. Bozano, S. Tuttle, S. A. Carter and P. J. Brock, *Appl. Phys. Lett.*, 1998, **73**, 3911.
21 B. Wang, H. Huang, A. B. Brennan and G. L. Wilkes, *Polym. Prepr. Div. Polym. Chem. ACS*, 1989, **30**(2), 146.
22 B. Wang and G. L. Wilkes, *J. Polym. Sci.: Part A, Polym. Chem.*, 1991, **29**, 905.
23 S. Wang, Z. Ahmad and J. E. Mark, *Chem. Mater.*, 1994, **6**, 943.
24 E. R. Kleinfeld and G. S. Ferguson, *Mater. Res. Soc. Symp. Proc.*, 1994, **351**, 419.
25 I. Ichinose, H. Senzu and T. Kunitake, *Chem. Lett.*, 1996, 831.
26 G. Decher, J. D. Hong and J. Schmitt, *Thin Solid Films*, 1992, **210**(211), 831.
27 J. H. Cheung, A. C. Fou and M. F. Rubner, *Thin Solid Films*, 1994, **244**, 895.
28 E. R. Kleinfeld and G. S. Ferguson, *Science*, 1994, **265**, 370.
29 Y. Liu, A. Wang and R. O. Claus, *Appl. Phys. Lett.*, 1997, **71**(16), 2265.
30 A. C. Fou and M. F. Rubner, *Macromolecules*, 1995, **28**, 7115.
31 D. Laurent and J. B. Schlenoff, *Langmuir*, 1997, **13**(6), 1552.
32 M. Raposo, R. S. Pontes, L. H. C. Mattoso and O. N. Oliveira Jr., *Macromolecules*, 1997, **30**(29), 6095.
33 N. Sato, M. Rikukawa, K. Sanui and N. Ogata, *Synth. Met.*, 1999, **101**, 132.
34 M. K. Ram, M. Salerno, M. Adami, P. Faraci and C. Nicolini, *Langmuir*, 1999, **15**, 1252.
35 A. T. Royappa and M. F. Rubner, *Langmuir*, 1992, **8**, 3168.
36 B. P. Meyer, B. W. Pfenning, J. P. Schoonover, C. J. Timpson, J. F. Wall, C. Kobusch, X. Chen, B. M. Deek, C. G. Wall, W. Ou, B. W. Erichson and C. A. Bignozzi, *Inorg. Chem.*, 1994, **33**, 3952.
37 H. Shin, R. J. Collins, M. R. De Jguire, A. H. Heuer and C. N. Sukenik, *J. Mater. Res.*, 1995, **10**, 692.
38 G. A. Neff, M. R. Helfrich, M. C. Clifton and C. J. Page, *Chem. Mater.*, 2000, **12**, 2363.
39 A. Hatzor, T. van der Boom-Moav, S. Yochelis, A. Vaskevich, A. Shanzer and I. Rubinstein, *Langmuir*, 2000, **16**(10), 4420.
40 I. Ichinose, T. Kawakami and T. Kunitake, *Adv. Mater.*, 1998, **10**, 535.
41 M. A. Rodrigues, D. F. S. Petri, M. J. Politi and S. Brochsztain, *Thin Solid Films*, 2000, **371**, 109.
42 L. Brus, *J. Phys. Chem.*, 1986, **90**, 2555.
43 C. Kormann, D. W. Bahnemann and M. R. Hoffmann, *J. Phys. Chem.*, 1988, **92**, 5196.
44 H. Ding, V. Erokhin, M. K. Ram, P. Sergio and C. Nicolini, *Mater. Sci. Eng. C*, 2000, **11**(2), 121.
45 G. Sauerbrey, *Z. Phys.*, 1959, **155**, 206.
46 I. Ivanda, S. Musié, S. Popovié and M. Gotié, *J. Mol. Struct.*, 1999, **480–481**, 645.
47 J. Li and K. Aoki, *J. Electroanal. Chem.*, 1998, **458**, 155.
48 K. Kajihara, K. Tanaka, K. Hirao and N. Soga, *Jpn. J. Appl. Phys.*, 1997, **36**, 5537.